BRDF Anisotropy Criterion

Michal Haindl(✉) and Votěch Havlíček

The Institute of Information Theory and Automation of the ASCR, Prague, Czechia
{haindl,havlicek}@utia.cas.cz
http://www.utia.cas.cz

Abstract. Visual scene recognition is predominantly based on visual textures representing an object's material properties. However, the single material texture varies in scale and illumination angles due to mapping an object's shape. We present an anisotropy criterion of bidirectional reflectance distribution function (BRDF), which allows deciding if a simpler isotropic BRDF model can be used or if it is necessary to use a more complex anisotropic BRDF model. The criterion simultaneously shows dominant angular orientations for the anisotropic materials. The anisotropic criterion is tested on several isotropic and anisotropic surface materials, with BRDF computed from the measured seven-dimensional Bidirectional Texture Function.

Keywords: BRDF modeling · Anisotropy criterion · Hyperspectral BRDF

1 Introduction

A human observer recognizes a visual scene using shape and material attributes. Unfortunately, the surface material's appearance changes under variable observation conditions [10,19], negatively affecting its automatic and reliable recognition in numerous artificial intelligence applications. As a consequence, most material recognition attempts apply unnaturally restricted observation conditions [2,6,24].

An ideal model for representing and classifying materials should be capable of capturing fundamental perceptual materials' properties. A multidimensional visual texture is an appropriate paradigm for such a surface reflectance function model. The best measurable representation is the seven-dimensional Bidirectional Texture Function (BTF) [7]. BTF can be simultaneously measured and modeled, even if it is not a trivial task, using state-of-the-art measurement devices and computers and the most advanced visual data multidimensional mathematical models. Features derived from such multidimensional data models are information preserving because they can synthesize data spaces closely resembling the original measurement data space.

However, such an enormous amount of visual BTF data, in the range of terabytes, measured on a single material sample, inevitably requires state-of-the-art storage, compression, modeling, visualization, and quality verification.

The Czech Science Foundation project GAČR 19-12340S supported this research.

N. T. Nguyen et al. (Eds.): ACIIDS 2022, LNAI 13758, pp. 434–444, 2022.
https://doi.org/10.1007/978-3-031-21967-2_35

Storage technology is still the weak part of computer technology, which lags behind recent data sensing technologies; thus, even for virtual reality correct materials modeling, it is infeasible to use BTF measurements directly, and often they are replaced with simplified BRDF model approximations.

The Bidirectional Reflectance Distribution function (BRDF) [7–9] is a simplified model which describes a material reflectance dependence on illumination and viewing angles while neglecting their spatial dependency, among others. However, this compromise allows improving realism in various graphics applications while it is far less computationally and memory demanding than the state-of-the-art Bidirectional Texture Function (BTF) representation. Various analytic BRDF models [1,3–5,11–18,20–23,25] were published primarily for isotropic materials, i.e., whose refection does not depend on the surface's orientation (rotation invariant). The modeling quality for anisotropic materials is usually significantly worse.

This paper's contribution is a novel anisotropy criterion, which allows deciding if a simpler isotropic BRDF model can be used or is necessary to use an anisotropic BRDF model. The criterion simultaneously shows dominant azimuthal orientations for the anisotropic materials. We present a comparative analysis with several isotropic and anisotropic materials from our extensive BTF database. For this analysis, we take advantage of the unique UTIA BTF visual material measurements [9].

2 Bidirectional Reflectance Distribution Function

A physically plausible BRDF must be non-negative (1), and it obeys the symmetry (2), and energy conservation properties (3):

$$BRDF(\lambda, \theta_i, \varphi_i, \theta_v, \varphi_v) > 0, \tag{1}$$

$$BRDF(\lambda, \theta_i, \varphi_i, \theta_v, \varphi_v) = BRDF(\lambda, \theta_v, \varphi_v, \theta_i, \varphi_i), \tag{2}$$

$$\int_{\Omega} BRDF(\lambda, \theta_i, \varphi_i, \theta_v, \varphi_v) \cos\theta_i d\omega_i \leq 1, \tag{3}$$

where θ_i, θ_v are illumination and viewing elevation angles, φ_i, φ_v are illumination and viewing azimuthal angles, $\omega_i = [\theta_i, \varphi_i]$, and λ is the spectral index. A BRDF can be isotropic or anisotropic. The anisotropic BRDF model depends on five variables

$$Y^{BRDF} = BRDF(\lambda, \theta_i, \varphi_i, \theta_v, \varphi_v), \tag{4}$$

while the isotropic, i.e., when the reflected light does not depend on surface orientation, only on four variables

$$Y^{BRDF} = BRDF(\lambda, \theta_i, |\varphi_i - \varphi_v|, \theta_v). \tag{5}$$

The BRDF models are mostly divided into two components - diffuse and specular. The diffuse component models equal light distribution into all angles, while the specular component assumes highly reflective blobs randomly distributed on the surface and influenced by the surface shape.

Numerous non-linear BRDF models were published, such as Binn model [3], Cook-Torrance model [4], Edwards model [5], Hapke - Lommel - Seeliger model [11], Lafortune model [12], Lewis model [13], Minnaert model [14], Oren-Nayar model [15,17], Phong model [18], Schlick model [20,21], stretched Phong model [16]. Other BRDF models are based on the microfacet theory Ashikhmin-Shirley [1], Torrance-Sparrow [22], Trowbridge-Reitz [23] and several others. Most BRDF models are restricted to isotropic materials and few models (e.g., [5,20,21,25] are capable to model anisotropic materials.

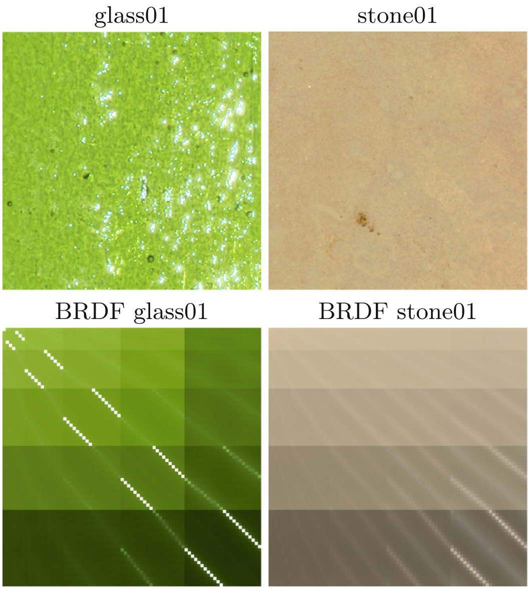

Fig. 1. Two tested isotropic materials and their corresponding BRDF.

3 Anisotropy Criterion

The suggested anisotropy criterion ε (11) depends on the selected range of BRDF measurements and can be applied to any number of spectral bands with a straightforward modification of the Eq. (11).

$$\boldsymbol{\varepsilon}(k) = \frac{1}{n(k)} \sum_{\forall \theta_i} \sum_{\forall \theta_v} \boldsymbol{\alpha}(\theta_i, \theta_v, k), \tag{6}$$

$$\boldsymbol{\varepsilon} = \frac{1}{n_k} \sum_{\forall k} \boldsymbol{\varepsilon}(k) = \frac{1}{n_k} \sum_{\forall k} \frac{1}{n(k)} \sum_{\forall \theta_i} \sum_{\forall \theta_v} \boldsymbol{\alpha}(\theta_i, \theta_v, k), \tag{7}$$

$$\boldsymbol{\alpha}(\theta_i, \theta_v, k) = |\boldsymbol{f}_{BRDF}(\theta_i, \theta_v, \phi_i, \phi_v) - \boldsymbol{\mu}_{BRDF}(\theta_i, \theta_v, k)|, \tag{8}$$

$$\boldsymbol{\mu}_{BRDF}(\theta_i, \theta_v, k) = \frac{1}{n_{\theta_i,\theta_v}(k)} \sum_{\forall \triangle\phi = k} \boldsymbol{f}_{BRDF}(\theta_i, \theta_v, k), \tag{9}$$

$$k = |\phi_i - \phi_v|, \tag{10}$$

$$\varepsilon = |\boldsymbol{\varepsilon}| = \sqrt{\sum_{\forall \lambda} \varepsilon_\lambda^2}, \tag{11}$$

$$\varepsilon = \sqrt{\varepsilon_R^2 + \varepsilon_G^2 + \varepsilon_B^2}, \tag{12}$$

where $n(k)$ is the number of all angular combinations for a specific k, n_k is the number of all possible differences k (i.e., $n_k = 226$ for 81×81 angular format), $\boldsymbol{\mu}_{BRDF}(\theta_i, \theta_v, k)$ (9). The anisotropy criterion for usual RGB color representation is (12). Spectral curves $f(\alpha(\lambda, \theta_i, \theta_v, k))$ denote anisotropy directions.

4 Experimental Textures

We tested the anisotropy criterion on our extensive UTIA BTF database [9] (Fig. 1), composed of material images under varying illumination and viewing directions. The anisotropy wood materials (Figs. 2, 3) were tested on the Wood UTIA BTF Database. All BRDF tables (Figs. 1, 2, 3 - bottom) were computed from the BTF measurements.

4.1 Wood UTIA BTF Database

The Wood UTIA BTF database contains veneers from sixty-five varied European, African, and American wood species. Among the European wood species are elm, fir, pear, pine, plum, birches, ash trees, cherry trees, larch, limba, linden, olive tree, spruces, beeches, oaks, walnuts, and maple trees. The others are various African and American wood species.

The UTIA BTF database[1] was measured using the high precision robotic gonioreflectometer [8], which consists of independently controlled arms with a camera and light. Its parameters, such as angular precision of 0.03°, the spatial resolution of 1000 DPI, or selective spatial measurement, classify this gonioreflectometer as a state-of-the-art device. The typical resolution of the area of

[1] http://btf.utia.cas.cz/.

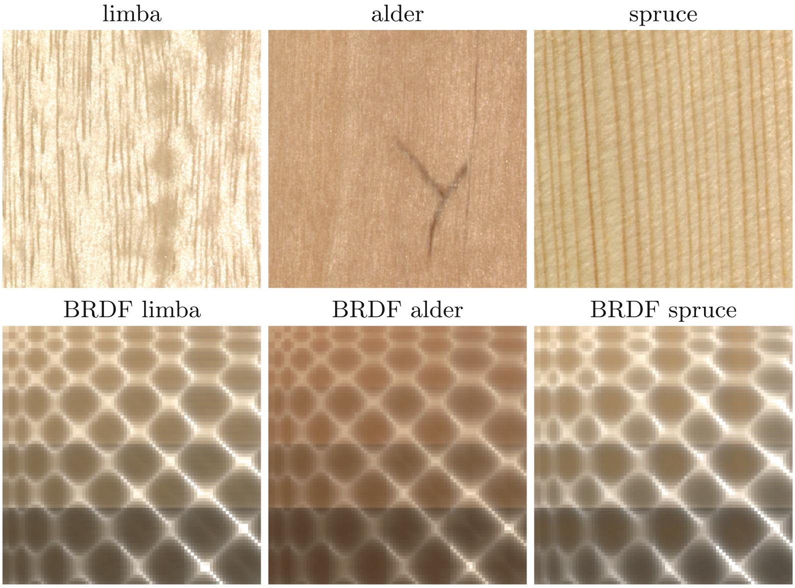

Fig. 2. Tested wood anisotropic materials and their corresponding BRDF.

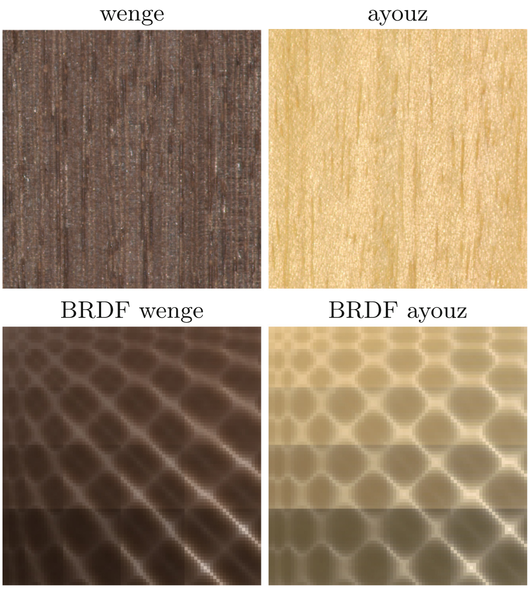

Fig. 3. Tested wood anisotropic materials and their corresponding BRDF.

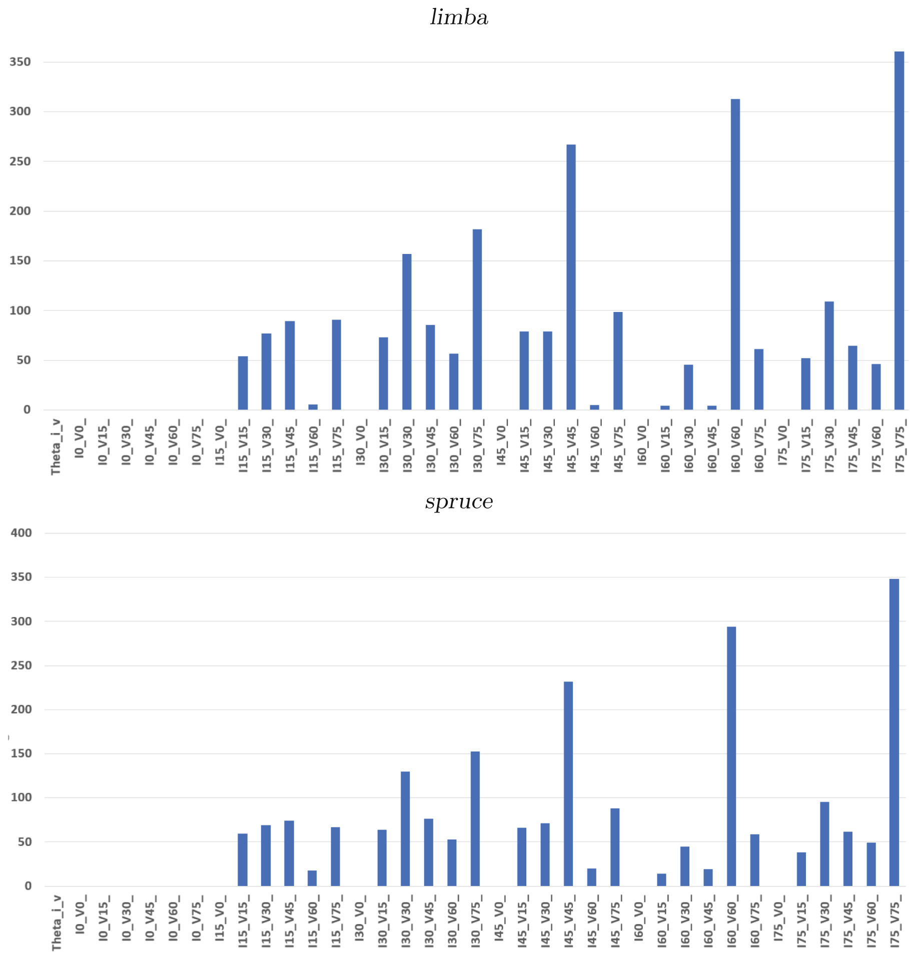

Fig. 4. Anisotropy criterion dependence on illumination and viewing elevation angles for limba and spruce anisotropic BRDF. The horizontal axis shows illumination (Ix θ_i) and viewing (_Vx θ_v) elevation angle combinations.

interest is around 2000×2000 pixels, sample size 7×7 [cm]. We measured each material sample in 81 viewing positions times 81 illumination positions resulting in 6561 images per sample, 4 TB of data. The images uniformly represent the space of possible illumination and viewing directions.

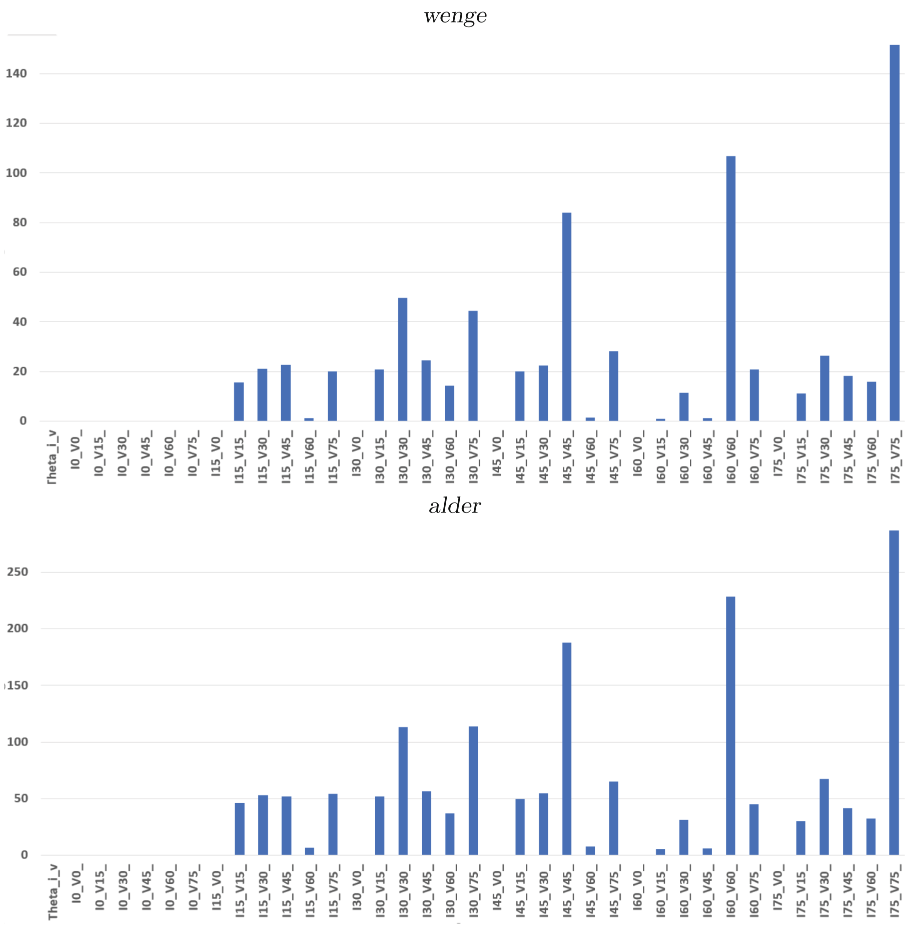

Fig. 5. Anisotropy criterion dependence on illumination and viewing elevation angles for wenge and alder anisotropic BRDF.

5 Results

Figures 1, 2, 3 - upper rows show presented materials for viewing and illumination angles approximately collinear with the surface normal. The visual evaluation suggests azimuthal independence for isotropic glass and stone materials on Fig. 1 while strong dependence on azimuthal angles for anisotropic limba and spruce wood on Fig. 2. The remaining three anisotropic wood materials (alder, ayouz, and wenge) also depend on azimuthal angles but not so noticeably.

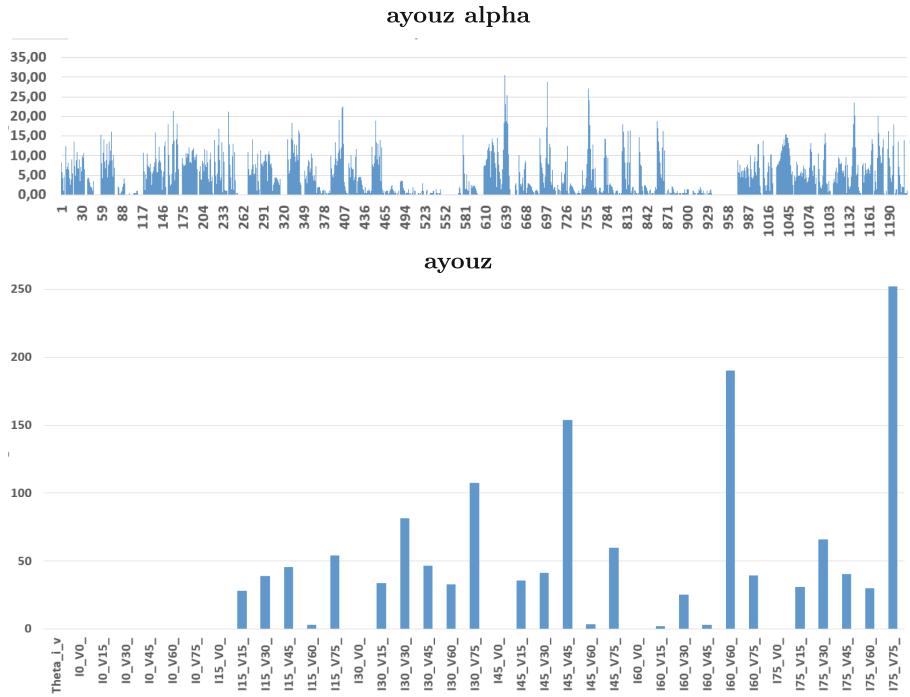

Fig. 6. $\alpha(\theta_i, \theta_v, k)$ curve for the B spectral channel and anisotropy criterion dependence on illumination and viewing elevation angles for ayouz anisotropic BRDF.

Table 1 summarizing anisotropy criterion values $\boldsymbol{\varepsilon}$ (7), ε (11) for all presented isotropic and anisotropic materials confirms the above visual observation. The largest criterion value, 30, has the most anisotropic spruce wood, while the isotropic stone and green glass values are only 1.76 and 5.48, respectively. The more considerable criterion value for glass is due to its specular reflections, which do not exist in diffuse stone material (Fig. 1). Smaller criterion values are for less highlighted anisotropy for wenge, ayouz (Fig. 3), and alder (Fig. 2 - middle) than for accentuated anisotropy for limba and spruce wood. Single spectral components ε_λ are very similar for related material. The materials ordering for our seven materials based on the criterion (stone, glass, wenge, ayouz, alder, limba, spruce) is identical using any spectral band λ in ε_λ or ε. Their standard deviation over the criterion spectral components is in the range $\langle 0.05; 1.85 \rangle$. The smaller the ε value, the smaller the modeling error can be expected from an isotropic BRDF model.

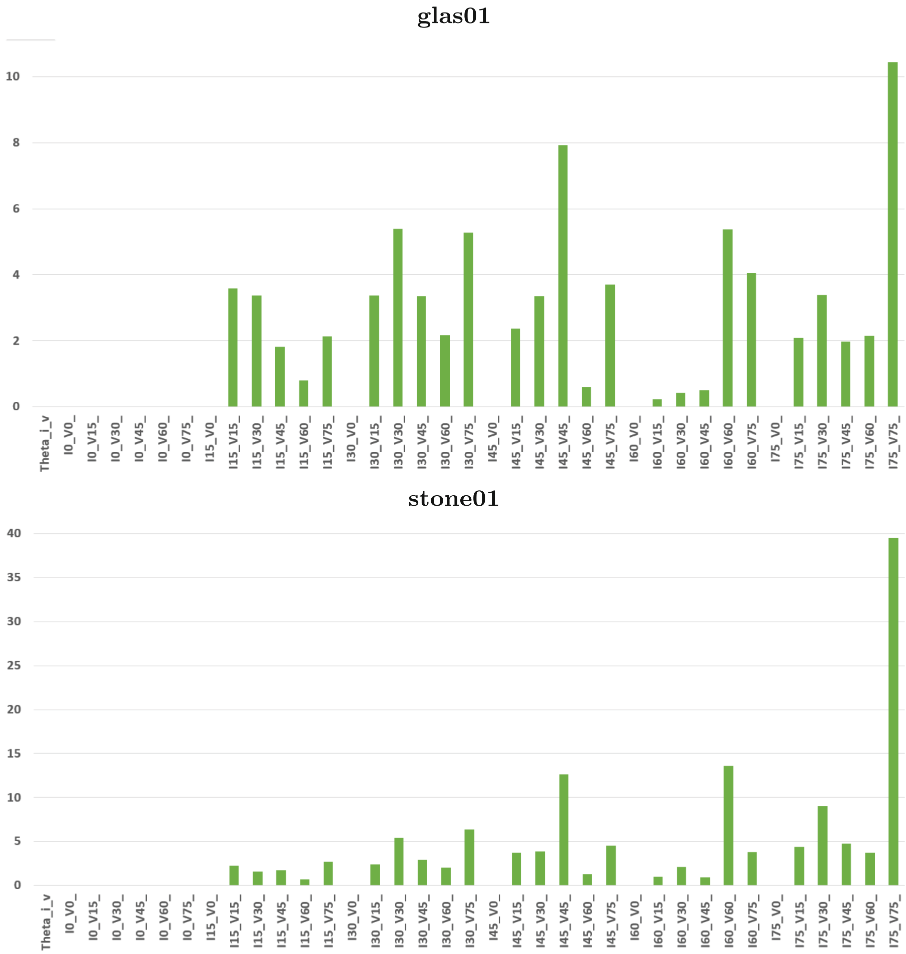

Fig. 7. Anisotropy criterion dependence on illumination and viewing elevation angles for glass01 and stone01 isotropic BRDF.

Anisotropy criterion graphical dependence on illumination and viewing elevation angles (horizontal axis) on Figs. 4, 5, 6 and 7 illustrates the above observation. The isotropic materials (Fig. 7) have small values in the range of tens, whereas the anisotropic wood materials (Figs. 4, 5 and 6) have these values in the range of hundreds.

Table 1. Anisotropy criterion

	glass01	stone0	wood05 ayouz	wood35 limba	wood45 alder	wood57 spruce	wood65 wenge
ε	2.96	1.08	7.76	12.71	8.25	15.06	5.62
	3.19	0.99	7.83	13.99	9.73	17.31	5.39
	3.60	0.97	8.36	15.30	10.02	19.06	5.33
ε	5.48	1.76	13.84	24.32	16.22	30.18	9.44
std	0.32	0.05	0.27	1.06	0.78	1.85	0.13

6 Conclusion

The anisotropy criterion of bidirectional reflectance distribution function allows deciding if a simpler isotropic BRDF model will provide sufficient quality modeling or if it is necessary to use a more complex anisotropic BRDF model. The criterion simultaneously shows dominant angular orientations for the anisotropic materials.

The presented results indicate that the anisotropic criterion can reliably differentiate between isotropic and anisotropic materials and thus can be used to select the appropriate class of BRDF nonlinear models. The criterion can be easily used for high-dynamic or hyperspectral measurements with a straightforward modification to any number of spectral bands.

References

1. Ashikhmin, M., Shirley, P.: An anisotropic phong BRDF model. J. Graph. Tools **5**(2), 25–32 (2000)
2. Bell, S., Upchurch, P., Snavely, N., Bala, K.: Material recognition in the wild with the materials in context database. In: Proceedings of the IEEE Conference on Computer Vision and Pattern Recognition, pp. 3479–3487 (2015)
3. Blinn, J.F.: Models of light reflection for computer synthesized pictures. In: Proceedings of the 4th Annual Conference on Computer Graphics and Interactive Techniques, pp. 192–198. ACM Press (1977)
4. Cook, R.L., Torrance, K.E.: A reflectance model for computer graphics. ACM Trans. Graph. (TOG) **1**(1), 7–24 (1982)
5. Edwards, D., et al.: The halfway vector disk for BRDF modeling. ACM Trans. Graph. (TOG) **25**(1), 1–18 (2006)
6. Gibert, X., Patel, V.M., Chellappa, R.: Material classification and semantic segmentation of railway track images with deep convolutional neural networks. In: 2015 IEEE International Conference on Image Processing (ICIP), pp. 621–625. IEEE (2015)
7. Haindl, M., Filip, J.: Visual Texture. Advances in Computer Vision and Pattern Recognition, Springer, London (2013). https://doi.org/10.1007/978-1-4471-4902-6, https://link.springer.com/book/10.1007/978-1-4471-4902-6

8. Haindl, M., Filip, J., Vávra, R.: Digital material appearance: the curse of tera-bytes. ERCIM News (90), 49–50 (2012). https://ercim-news.ercim.eu/en90/ri/digital-material-appearance-the-curse-of-tera-bytes
9. Haindl, M., Mikeš, S., Kudo, M.: Unsupervised surface reflectance field multi-segmenter. In: Azzopardi, G., Petkov, N. (eds.) CAIP 2015. LNCS, vol. 9256, pp. 261–273. Springer, Cham (2015). https://doi.org/10.1007/978-3-319-23192-1_22
10. Haindl, M., Vácha, P.: Wood veneer species recognition using Markovian textural features. In: Azzopardi, G., Petkov, N. (eds.) CAIP 2015. LNCS, vol. 9256, pp. 300–311. Springer, Cham (2015). https://doi.org/10.1007/978-3-319-23192-1_25
11. Hapke, B.W.: A theoretical photometric function for the lunar surface. J. Geophys. Res. **68**(15), 4571–4586 (1963)
12. Lafortune, E., Foo, S., Torrance, K., Greenberg, D.: Non-linear approximation of reflectance functions. In: ACM SIGGRAPH 1997, pp. 117–126. ACM Press (1997)
13. Lewis, R.R.: Making shaders more physically plausible. In: Computer Graphics Forum, vol. 13, pp. 109–120. Wiley Online Library (1994)
14. Minnaert, M.: The reciprocity principle in lunar photometry. Astrophys. J. **93**, 403–410 (1941)
15. Nayar, S.K., Oren, M.: Visual appearance of matte surfaces. Science **267**(5201), 1153–1156 (1995)
16. Neumann, L., Neumannn, A., Szirmay-Kalos, L.: Compact metallic reflectance models. In: Computer Graphics Forum, vol. 18, pp. 161–172. Wiley Online Library (1999)
17. Oren, M., Nayar, S.K.: Generalization of lambert's reflectance model. In: Proceedings of the 21st Annual Conference on Computer Graphics and Interactive Techniques, pp. 239–246 (1994)
18. Phong, B.T.: Illumination for computer generated pictures. Commun. ACM **18**(6), 311–317 (1975)
19. Remeš, V., Haindl, M.: Bark recognition using novel rotationally invariant multi-spectral textural features. Pattern Recogn. Lett. **125**, 612–617 (2019)
20. Schlick, C.: A customizable reflectance model for everyday rendering. In: Fourth Eurographics Workshop on Rendering, Paris, France, pp. 73–83 (1993)
21. Schlick, C.: An inexpensive BRDF model for physically-based rendering. In: Computer graphics forum, vol. 13, pp. 233–246. Wiley Online Library (1994)
22. Torrance, K.E., Sparrow, E.M.: Off-specular peaks in the directional distribution of reflected thermal radiation. J. Heat Transf. **6**(7), 223–230 (1966)
23. Trowbridge, T., Reitz, K.P.: Average irregularity representation of a rough surface for ray reflection. JOSA **65**(5), 531–536 (1975)
24. Varma, M., Zisserman, A.: A statistical approach to material classification using image patch exemplars. IEEE Trans. Pattern Anal. Mach. Intell. **31**(11), 2032–2047 (2009). http://doi.ieeecomputersociety.org/10.1109/TPAMI.2008.182
25. Ward, G.: Measuring and modeling anisotropic reflection. Comput. Graph. **26**(2), 265–272 (1992)